DETECTION OF PLANT HORMONE ABSCISIC ACID (ABA) USING AN OPTICAL APTAMER-BASED SENSOR WITH A MICROFLUIDICS CAPILLARY INTERFACE

Chao Song[1], Changtian Chen[2], Xiangchen Che[1], Wei Wang[2], and Long Que[1]
[1]Electrical & Computer Engineering Department, Iowa State University, USA
[2]Plant Pathology & Microbiology Department, Iowa State University, USA

ABSTRACT

This paper reports, for the first time, an optical aptamer-based plant hormone sensor with a microfluidics capillary interface. The ssDNA aptamer-based sensor has better sensitivity with excellent specificity for detecting abscisic acid (ABA) than the ELISA detection kit from Sigma, indicating its potential for screening different plant hormones in a complicated matrix. Additionally, its microfluidics capillary interface allows the samples to be delivered to the sensor automatically without any external pumps, paving a way for its point-of-care application in the field.

INTRODUCTION

Most physiological and development processes in plants are regulated by plant hormones, which are small molecular natural products, including auxins, cytokinins, gibberellins (GA), abscisic acid (ABA), ethylene, etc. [1]. It is important to quantitatively analyze plant hormones for in-depth study of their biosynthesis, transport, metabolism and molecular regulatory mechanisms. Current widely-used laboratory procedures for detecting plant hormones include radioimmunoassay, enzyme linked immunosorbent assay (ELISA), chromatography and chromatography/mass spectrometry [1-3]. But these methods usually require skilled personnel and long-time analysis with high cost, hence are not suitable for point-of-care (POC) testing in the field. Electrochemical techniques, which can be utilized to develop microdevices, are an alternative approach due to their simplicity, convenience and low cost [1]. However, poor stability and reproducibility are hurdles to their wide application in practice. Nowadays, electrochemical biosensors remain at the early stage of methodology probes for detecting plant hormones. Herein, an optical aptamer-based sensor with a capillary microfluidics interface is reported.

DEVICE DESCRIPTION, FABRICATION & TESTING

Operational principle

The sketch of the proposed chip and its operational principle are illustrated in Fig. 1. The chip (Fig. 1a) consists of a nanopore-sensing region and SU8 micro-structures at its upstream and downstream, which are integrated as capillary microfluidics. After the samples are delivered to the chip, the samples will be automatically transported to the nanopore-sensing region by the capillary force by the SU8 micro-structures (Fig. 1b) [4-5]. At the downstream of the chip close to the nanopore-sensing region, some passive valves are integrated to prevent the chemicals from flowing out of the sensing region. If the sensing region needs to be rinsed, buffer solution will be flowed into the capillary microfluidics, which are integrated at the upstream and downstream of the passive valves (Fig.1b-c). By this way, the samples can be delivered to the sensing region and the chip can also be cleaned automatically without any external pumps.

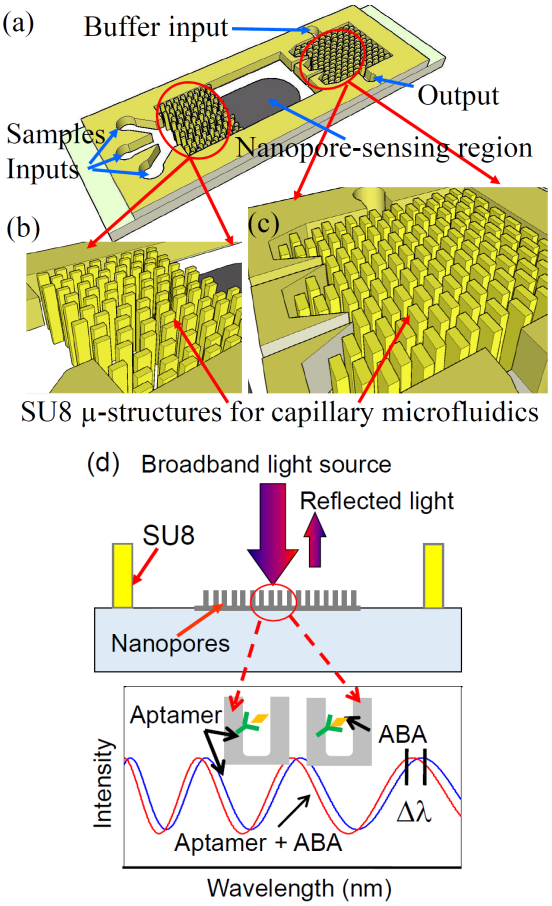

Figure 1: (a) Sketch of the sensor chip; (b-c) close-up showing the SU8 microstructures for microfluidics capillary interface; (d) the optical transducing signal from the nanopore-sensing region: optical interface fringes peak shift before and after ABA is bound to its aptamer.

The optical interference fringes reflected from the nanopore-sensing region is the transducing signal (Fig. 1d) [6-7]. The sensing region is an anodic aluminum oxide (AAO) thin film, which consists of periodically distributed nanopores. Aptamer-based sensing is used [8], which offers a cost-effective platform with a very good temperature stability, and has a wide tolerance range of pH and salt concentration with a similar, if not better,

specificity and affinity to antibody-based sensing [9-10]. In addition, aptamers can also be reversibly denatured for the release of target molecules, hence the aptamer-based sensor can be reused. The aptamer-based sensing along with the microfluidics capillary interface makes the chip particularly suitable for low-cost POC application in the field.

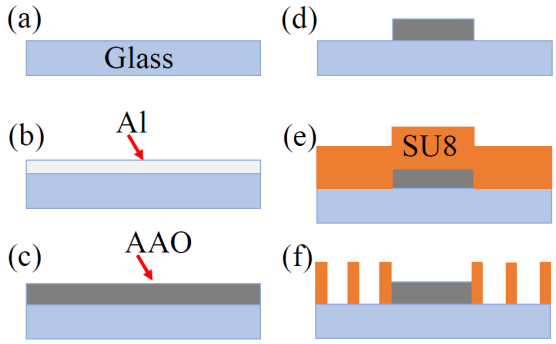

Figure 2: Process flow to fabricate the chip: Nanopore-sensing region with a SU8-based microfluidics capillary interface.

Chip fabrication

Figure 2 gives the process flow to fabricate the chip. Briefly, a nanopore-sensing region is patterned from anodic aluminum oxide (AAO) thin film [11], then a microfluidics capillary interface is fabricated from SU8, followed by bonding three PDMS slabs with inputs and outputs.

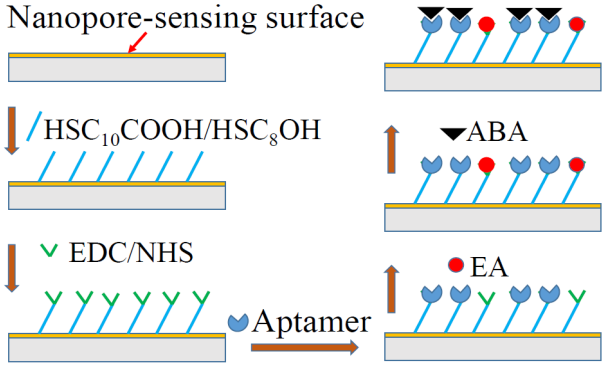

Figure 3: Surface functionalization procedure of the nanopore-sensing region for detecting ABA using ssDNA ABA aptamer.

Sensor surface functionalization

Figure 3 illustrates the sensor's surface functionalization procedure. The Au-coated sensor surface is functionalized with ABA aptamer through 1-ethyl-3-(3-dimethylaminopropyl) carbodiimide (EDC)/N-hydroxysulfosuccinimide (NHS) chemistry. Specifically, the Au-coated sensor surface is immersed in the 10 mM $HSC_{10}COOH/HSC_8OH$ solution overnight and then washed with PBS. After the surface is dried, the surface is immersed in a solution of NHS and EDC (NHS 0.2M, EDC 0.05M) for 2 hrs. The sensor surface is then washed with DI water and then immersed in the 2 µM ABA aptamer solution overnight. This is followed by loading of 100 µL 1 M ethanolamine (EA) to block the non-occupied HSC10COOH/HSC8OH sites activated by the EDC/NHS. Finally, the sensor surface is rinsed with the PBS buffer to flush off non-specifically adsorbed aptamer and other chemicals. At this stage, the sensor is ready for the measurement.

Testing setup and procedure

The testing setup is illustrated in Fig. 4, which is the similar to and has been described in detail in previous literatures [6-7].

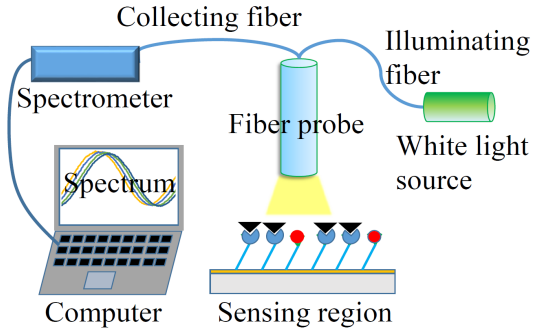

Figure 4: the optical setup for detecting the transducing signals in the sensing region of the chip.

For all the reported measurements in next section, after the samples are applied to the sensor and incubated for 30-50 min, three time rigorous rinse by running PBS buffer to remove the unbound samples on the sensor surface has been carried out, followed by three optical measurements. The results are the average values from the three measurements.

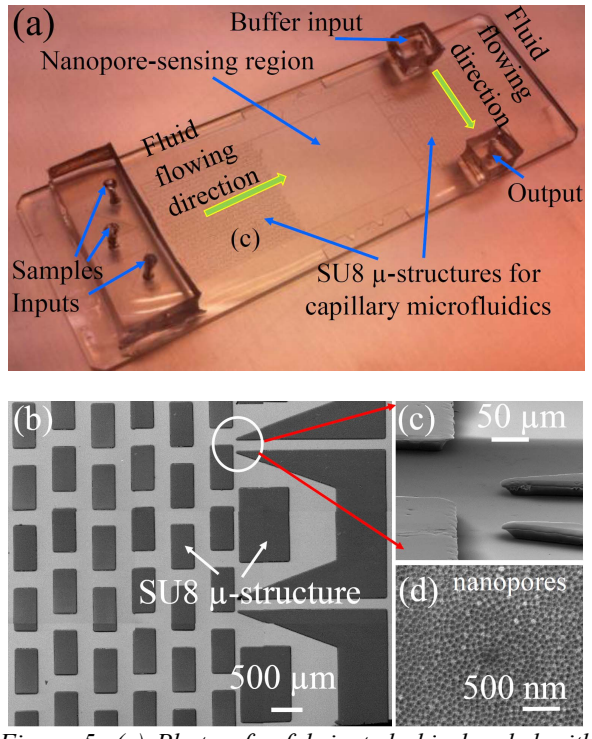

Figure 5: (a) Photo of a fabricated chip bonded with PDMS slabs with inputs and outputs; (b-d) SEM images of the SU8 microstructures for capillary microfluidics and the nanopore-sensing region fabricated from anodic aluminum oxide (AAO).

RESULTS AND DISCUSSION

Fabricated chip and demonstration of its functions

A photo of a fabricated sensor chip is shown in Fig. 5a. The SEM images of the SU8-based microfluidics capillary structures and the passive valves are given in Fig. 5b-c. The SEM image of the nanopore-sensing region, fabricated by anodizing the Al thin film, is shown in Fig. 5d. The thickness of SU8 microstructures is ~30 µm. The nanopore size is 40-50 nm.

The blue food dye, due to its clear visibility, is used to demonstrate the functions of the capillary microfluidics. The food dye is continuously filled into the inputs (Fig. 6). As a result, it is automatically flowed through the SU8 microstructures in Fig. 6a-b, arrives at the nanopore-sensing region (Fig. 6c), and finally reaches the passive valves and then stops flowing (Fig. 6d). It takes ~ 1 min for the whole process.

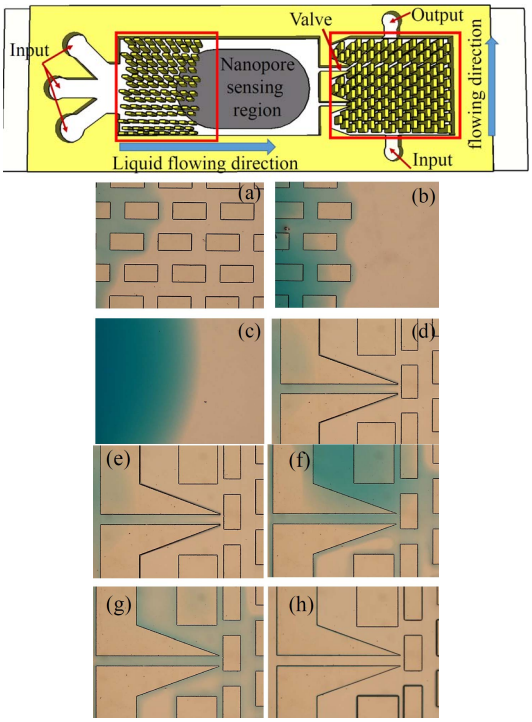

Figure 6: Demonstration of functions of the capillary microfluidics: (top) sketch of the chip; (a)-(b) food dye flows through the SU8 microstructures due the capillary force; (c) food dye reaches the nanopore-sensing region; (d) food dye reaches the passive valves; (e)-(f) water is flowed to the passive valves, the food dye is drained out of the nanopore sensing region; (h) food dye is washed out of the chip.

In order to make the blue food dye flow out of the passive valves, water is filled into the input of the capillary microfluidics at the downstream of the passive valves continuously. As a result, the food dye is drained out of the nanopore-sensing region (Fig. 6e-g). And eventually all the food dye is cleaned up from the chip (Fig. 6h). It takes ~ 1 min to complete the cleaning process.

ABA measurement

Figure 7 gives the sensing responses (shift of optical interference fringes) of the sensor for different concentrations of ABA in buffer. As its concentration increases from 0.1 µM to 10 µM, the shift of the optical interference fringes increases from 0.7 nm to 2.7 nm with a high linearity, resulting from the increased change of effective refractive index due to the increased binding of ABA with ABA aptamer.

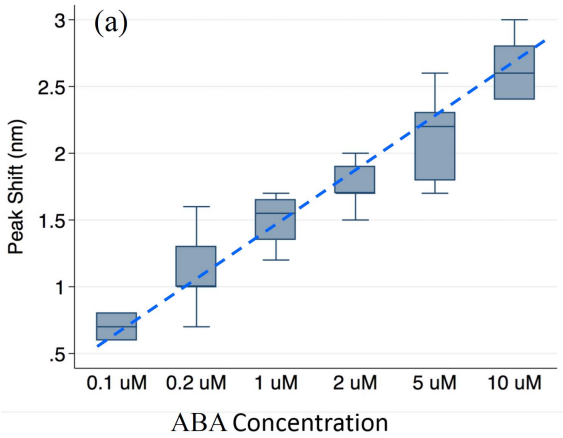

Figure 7: Measured responses for different concentrations of ABA in buffer solution, showing excellent linearity.

Using this sensor, ABA at a concentration of 0.1 µM can be readily detected, offering better detection limit and sensitivity than the ELISA based ABA detection kit from Sigma [12]. It is anticipated that the detection limit can be further improved by optimizing the performance of the nanopore-based sensor.

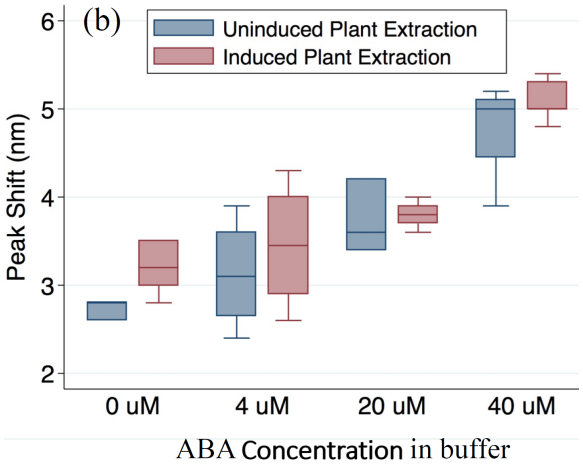

Figure 8: Measured responses for two types of samples of plant extractions with and without ABA inducing.

ABA measurement from plant extractions

In order to assess the endogenous ABA concentration changes from plant tissues with 1.5 mM $MgSO_4$ treatment which can induce ABA production [13], the ABA in two types of plant extractions has been tested. One is a sample without $MgSO_4$ treatment, the other is a sample with $MgSO_4$ treatment. The two types of samples were added to a series of buffers with different known ABA concentrations for measurements. As expected and shown

in Fig. 8, the ABA concentration increases for the induced plant extraction compared with the un-induced plant extraction. Based on the measurements, the quantities of the ABA in plant extractions can be determined.

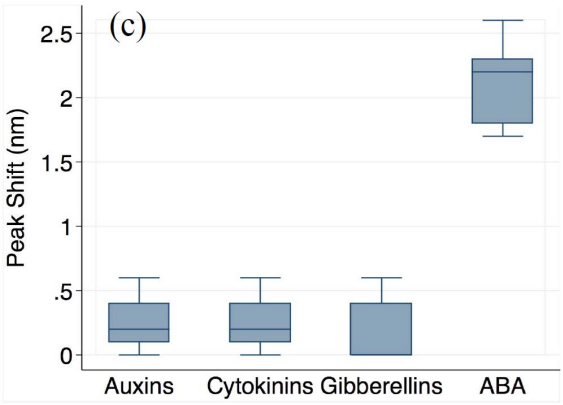

Figure 9: Measured responses for four plant hormones with the same concentration of 5 μM using four ABA aptamer functionalized sensors, showing excellent specificity.

Specificity evaluation

The specificity of the sensor was evaluated by detecting different hormones using the ABA aptamers. In these experiments, four sensors functionalized with the same concentration of ABA aptamer have been used to test four hormones at the same concentration of 5 μM, including auxins, cytokinins, gibberellins (GA), and abscisic acid (ABA). The measurements in Fig. 9 show that the optical signal shift is 0.44 nm, 0.26 nm and 0.2 nm for three other hormones (auxins, cytokinins, gibberellins) respectively, much smaller than 2.12 nm for ABA, indicating its excellent specificity and selectivity.

It should be noted that even though the non-specific binding for other hormones and other contents in plant extractions is small, but the optical fringe shift still exists (Fig. 8 & 9). In order to further cancel out the non-specific binding effect when detecting ABA in complex fluids, some reference sensors are needed to calibrate the shift due to the non-specific binding. Then, the pure shift due to the ABA can be obtained by subtracting the shift of the reference sensors from the measurements of the ABA in complex fluids.

SUMMARY

In this paper, an optical aptamer-based sensor to detect plant hormone ABA is reported. Experiments found that the detection limit of the sensor with excellent specificity is 0.1 μM, lower than that of the commercially available ELISA based ABA detection kit from Sigma. A capillary microfluidics interface integrated with the sensor allows the samples to be delivered to the sensor and also to be rinsed and flowed out of the sensor automatically without any external pumps, making the chip suitable for point-of-care applications in the field.

ACKNOWLEDGEMENTS

This effort was partly funded by a NSF grant. The mask layout for the capillary microfluidics by Ms. Silu Feng is appreciated.

REFERENCES

[1] J. Fu, X. Sun, J. Wang, J. Chu, C. Yan, "Progress in quantitative analysis of plant hormones," *Chinese Science Bulletin*, vol. 56(4-5), pp. 355-366, 2011.

[2] M. Müller, S. Munné-Bosch, "Rapid and sensitive hormonal profiling of complex plant samples by liquid chromatography coupled to electrospray ionization tandem mass spectrometry," *Plant methods*, vol. 7(1), pp. 1-11, 2011.

[3] X. Pan, R. Welti, X. Wang, "Quantitative analysis of major plant hormones in crude plant extracts by high-performance liquid chromatography–mass spectrometry," *Nature Protocols*, vol. 5(6), pp. 986-992, 2010.

[4] M. Zimmermann, H. Schmid, P. Hunziker, E. Delamarche, "Capillary pumps for autonomous capillary systems," *Lab on a Chip*, vol. 7(1), pp. 119-125, 2007.

[5] F. Zang, K. Gerasopoulos, K. McKinzie, J. N. Culver, and R. Ghodssi, "Autonomous capillary microfluidics for rapid nanoreceptor assembly and biosensing," In *18th International Conference on Solid-State Sensors, Actuators and Microsystems* (TRANSDUCERS 15), pp. 548-551. IEEE, 2015.

[6] T. Zhang, Z. Gong, R. Giorno, L. Que, "A nanostructured Fabry-Perot interferometer," *Optics Express*, vol. 18, no. 19, pp. 20282-20288, 2010.

[7] T. Zhang, P. Pathak, S. Karandikar, R. Giorno, and L. Que, "A polymer nanostructured Fabry-Perot interferometer based biosensor," *Biosensors and Bioelectronics*, vol. 30(1), pp.128-132, 2011.

[8] S. Feng, C. Chen, X. Che, W. Wang, and L. Que, "Rapid detection of theophylline using aptamer-based nanopore thin film sensor," *Proc. IEEE Sensors Conference*, pp. 1658-1660, 2016.

[9] S. Alzghoul, M. Hailat, S. Zivanovic, L. Que, G. Shah, "Measurement of serum prostate cancer biomarkers using a nanopore thin film based optofluidic chip," *Biosensors and Bioelectronics*, vol. 77, pp. 491-498, 2016.

[10] T. Zhang, Y. He, J. Wei and L. Que, "Nanostructured optical microchips for cancer biomarker detection," *Biosensors and Bioelectronics*, vol. 38(1), pp. 382-388, 2012.

[11] H. Yin, X. Li and L. Que, "Fabrication and characterization of the arrayed aluminum oxide thin film micropatterns on glass substrate," *Microelectronic Engineering*, vol. 128, pp. 66-70, 2014.

[12] http://www.sigmaaldrich.com/catalog/product/sigma/pgr1?lang=en&region=US

[13] M. Cao, Z. Wang, Q. Zhao, J. Mao, A. Speiser, M. Wirtz, C. Xiang, "Sulfate availability affects ABA levels and germination response to ABA and salt stress in Arabidopsis thaliana," *The Plant Journal*, vol.77(4), pp. 604-615, 2014.

CONTACT

*L. Que, tel: +1-515-294-6951; lque@iastate.edu